REPORT DOCUMENTATION PAGE

Form Approved
OMB No. 0704-0188

1. REPORT DATE *(DD-MM-YYYY)*	2. REPORT TYPE	3. DATES COVERED *(From - To)*
28 March 2003	Technical Paper	

4. TITLE AND SUBTITLE

First-Principles Calculations of the Adsorption of Nitromethane and 1,1-Diamino-2, 2-dinitroethlene (FOX-7) Molecules on the A1(111) Surface

5a. CONTRACT NUMBER

5b. GRANT NUMBER

5c. PROGRAM ELEMENT NUMBER

6. AUTHOR(S)
Dan C. Sorescu[1], Jerry A. Boatz[2], Donald L. Thompson

5d. PROJECT NUMBER
2303

5e. TASK NUMBER
M2C8

5f. WORK UNIT NUMBER

7. PERFORMING ORGANIZATION NAME(S) AND ADDRESS(ES)

[1]U.S. Department of Energy
National Energy Technology Laboratory
P.O. Box 10940
Pittsburgh, PA 15236

[2]Air Force Research Laboratory (AFMC)
AFRL/PRSP
10 E. Saturn Blvd.
Edwards AFB, CA 93524-7680

8. PERFORMING ORGANIZATION REPORT NUMBER

AFRL-PR-ED-TP-2003-075

9. SPONSORING / MONITORING AGENCY NAME(S) AND ADDRESS(ES)

Air Force Research Laboratory (AFMC)
AFRL/PRS
5 Pollux Drive
Edwards AFB CA 93524-7048

10. SPONSOR/MONITOR'S ACRONYM(S)

11. SPONSOR/MONITOR'S NUMBER(S)
AFRL-PR-ED-TP-2003-075

12. DISTRIBUTION / AVAILABILITY STATEMENT

Approved for public release; distribution unlimited.

13. SUPPLEMENTARY NOTES

14. ABSTRACT

15. SUBJECT TERMS

16. SECURITY CLASSIFICATION OF:			17. LIMITATION OF ABSTRACT	18. NUMBER OF PAGES	19a. NAME OF RESPONSIBLE PERSON
a. REPORT	b. ABSTRACT	c. THIS PAGE			Sheila Benner
Unclassified	Unclassified	Unclassified	A		19b. TELEPHONE NUMBER *(include area code)* (661) 275-5963

FILE

MEMORANDUM FOR PRS (In-House Publication)

31 Mar 2003

FROM: PROI (STINFO)

SUBJECT: Authorization for Release of Technical Information, Control Number: **AFRL-PR-ED-TP-2003-075**
Dan C. Sorescu (US DOE Nat'l Energy Tech Lab); Jerry A. Boatz (AFRL/PRSP); Donald L. Thompson (OK State Univ), "First-Principles Calculations of the Adsorption of Nitromethane and 1,1-Diamino-2,2-dinitroethylene (FOX-7) Molecules on the Al(111) Surface"

Boatz 5364

DoD User's Group Conference Proceedings, Journal of Physical Chemistry **(Statement A)**
(Bellevue, WA, 9-13 Jun 2003) **(Deadline: 09 Jun 2003)**

First-Principles Calculations of the Adsorption of Nitromethane and 1,1-Diamino-2,2-dinitroethylene (FOX-7) Molecules on the Al(111) Surface

Dan C. Sorescu,* Jerry. A. Boatz** and Donald L. Thompson***

* U. S. Department of Energy, National Energy Technology Laboratory, P. O. Box 10940, Pittsburgh, PA 15236 and Department of Chemical and Petroleum Engineering, University of Pittsburgh, Pittsburgh, PA 15260

** Air Force Research Laboratory, AFRL/PRSP, Edwards AFB, CA 93524

*** Department of Chemistry, Oklahoma State University, Stillwater, OK 74078

ABSTRACT

First-principles calculations based on spin-polarized density functional theory (DFT) and the generalized gradient approximation (GGA) have been used to study the adsorption of nitromethane (NM) and 1,1-diamino-2,2-dinitroethylene (FOX-7) molecules on the Al(111) surface. The calculations employ (3x3) aluminum slab geometries and 3D periodic boundary conditions. Based on these calculations, we have determined that both dissociative and nondissociative adsorption mechanisms are possible, depending on the molecular orientation and the particular surface sites involved. In the case of dissociative chemisorption, O abstraction by Al surface atoms is seen to be the dominant mechanism. The dissociated oxygen atom forms strong Al-O bonds with the neighboring Al sites around the dissociation sites. Additionally, the radical species obtained as a result of oxygen atom elimination remains bonded to the surface. In some instances, both oxygen atoms of the nitro group dissociate and oxidize the aluminum surface. Finally, for the case of nondissociative adsorption, various N-O-Al bridge-type bonding configurations can be formed. Based on the data provided from these studies, it can be concluded that oxidation of the aluminum surface readily occurs, either by partial or complete dissociation of the oxygen atoms from the NO_2 group.

I. Introduction

Powderized aluminum has long been used as an energetic ingredient in rocket propellant formulations, comprising approximately 15-20% of conventional ammonium perchlorate solid propellant.[1] Its primary roles are to increase the combustion exothermicity and the regression rate of solid propellant grains and to enhance the blasting effect of explosives. Such properties are significantly affected by the size of the Al particles. For example, in the case of Al nanopowders, significant improvements in the performance of some energetic materials over the common micron-size Al powders have been reported.[2,3]

An important performance issue, particularly for nanoscale aluminum powders, is the formation of an aluminum oxide overcoat prior to combustion which inhibits efficient burning. When the thickness of the oxide overcoat is large, its presence severely reduces the potential advantages of using such high surface area-to-volume ratio ultrafine aluminum particles. Consequently, identification of new methods for passivation of Al particles to reduce the size of the oxide layer, without incurring a significant decrease in performance, are being considered. For example, it has been suggested to coat the aluminum particles with an energetic material such as hexahydro-1,3,5-trinitro-*s*-triazine (RDX).[4]

Currently, no experimental evidence is available to clarify the efficiency of passivation of Al nanoparticles when coated with various energetic materials. Moreover, a clear mechanism to describe the interaction of energetic materials (nitro compounds in particular), with Al surfaces is lacking. In order to clarify some of the fundamental issues related to the role played by energetic materials when deposited on an aluminum surface, the present work focuses on the atomic-level description of the interactions between the energetic compounds nitromethane (NM) and 1,1-diamino-2,2-dinitroethylene (FOX-7) with the Al(111) surface. Specifically, first-principles quantum chemical calculations are used to determine the chemisorption properties of the nitro-containing compounds of interest for energetic materials applications on aluminum surfaces.

II. Computational Method

The calculations performed in this study were done using the Vienna *ab initio* simulation package (VASP).[5-7] This program evaluates the total energy of periodically repeating geometries based on density-functional theory and the pseudopotential approximation. The electron-ion interaction is described by fully non-local optimized ultrasoft pseudopotentials similar to those introduced by Vanderbilt.[8,9] Periodic boundary conditions are used, with the one electron pseudo-orbitals expanded over a plane-wave basis set. The expansion includes all plane waves whose kinetic energy, $\eta^2 k^2 / 2m < E_{cut}$ where k is the wave vector, m the electronic mass and E_{cut} is the chosen cutoff energy. In this study a cutoff energy of 395 eV is chosen which ensures the convergence with respect to the basis set.

Calculations were performed using spin-polarized generalized gradient approximation (GGA) density functional theory using PW91 exchange-correlation functional.[10] The sampling of the Brillouin zone was performed using a Monkhorst-Pack scheme.[11] We have also used the Methfessel-Paxton technique[12] with a smearing of σ=0.2 eV in order to minimize the errors in the Hellmann-Feynman forces due to the entropic contribution to the electronic free energy.[5,6] All energies are extrapolated to T=0 K.

The minimization of the electronic free energy was performed using an efficient iterative matrix-diagonalization routine based on a sequential band-by-band residuum minimization method (RMM),[5,6] or alternatively based on preconditioned band-by-band conjugate-gradient (CG) minimization.[13] The optimization of different atomic configurations was performed by conjugate-gradient minimization of the total energy.

The Al surface is represented by a slab model with periodic boundary conditions applied in all three directions. Particularly, a 3x3 supercell with four layers containing 36 Al atoms is used to study the adsorption of various molecular systems. The slabs were separated by 10 Å and 15 Å of vacuum for the cases of NM and FOX-7 molecules, respectively. In calculations of molecular adsorption on the surface, we have relaxed all atomic positions of the molecule as well as the Al atoms located in the first layer of the slab.

III. Results and Discussion

A. Test Calculations for Bulk Al and isolated NM and FOX-7 molecules

A number of tests have been initially performed to verify the accuracy of the method when applied to bulk Al and to the isolated NM and FOX-7 molecules, and to clarify different technical aspects such as the optimum cutoff energy for calculations.

For bulk Al, we have tested for convergence the k-point sampling density as well as the kinetic energy cutoff. In these calculations a Monkhorst-Pack grid of 12x12x12 has been used, leading to 56 k-points in the irreducible Brillouin zone. In order to determine the equilibrium bulk parameters of Al we have uniformly scaled the lattice vectors and performed energy calculations as a function of unit cell volume. The calculated data were then fit with the Murnaghan equation of state.[14] The calculated lattice constant was found to be 4.044 Å, which differs by –0.14% from the corresponding experimental value of 4.050 Å.[15] The corresponding bulk modulus and its pressure derivative were found to be B_0=72.2 GPa and B_0'=4.16, respectively. These values differ, respectively, by –4.87% and –2.57% from the corresponding values of 75.9 GPa and 4.27, estimated in Ref. 16 based on the reported elastic constants of Al. These values indicate that the present set of pseudopotentials is able to provide a very good representation of the structural properties of bulk Al.

An equally good representation has been observed for the geometric parameters of the isolated NM and FOX-7 molecules. For example, based on optimizations of the isolated NM molecule in a cubic box of 12x12x12 $Å^3$, we have determined the following equilibrium bond lengths: r(C-N)=1.497 Å, r(N-O)=1.240 Å, and r(C-H)=1.090 Å, and bond angles θ(N-C-H)=106.6° and θ(N-O-N)=125.6°. These values are very close to those we have reported previously[17] for the isolated NM molecule based on hybrid density functional theory calculations at the B3LYP/6-31G** theoretical level. Additionally, the calculated values are also close to the experimental data for gas phase nitromethane.[18] In this case the largest deviation of 1.3% is seen for N-O bonds (r^{exp}(N-O)=1.224 Å).

For the case of the FOX-7 molecule, we have shown in a previous study[19] that plane-wave DFT calculations using the VASP code provide an accurate description of the structural properties of this molecule as well as the corresponding crystal structure. The

corresponding analysis will not be repeated here. The good agreement between our calculated properties of bulk Al and the isolated NM and FOX-7 molecules with experiment and/or previous theoretical predictions made us confident to proceed to the next step, *i.e.*, investigation of molecular adsorption on the Al(111) surface.

B. Nitromethane Adsorption on Al(111) Surface.

B1. Geometries and Energies

The adsorption of NM, which is a prototype for larger energetic molecules such as hexahydro-1,3,5-trinitro-*s*-triazine (RDX) or octahydro-1,3,5,7-tetranitro-1,3,5,7-tetrazocine (HMX), on the Al(111) surface was examined in detail for several distinct orientations of NM relative to the metallic surface. For the case of non-dissociative adsorption configurations, the corresponding adsorption energy was calculated according to the expression

$$E_{ads}=E_{molec} + E_{slab} - E_{(molec+slab)} \quad (1)$$

where E_{molec} is the energy of the isolated NM molecule in its equilibrium position, E_{slab} is the total energy of the slab and $E_{(molec+slab)}$ is the total energy of the adsorbate/slab system. A positive E_{ads} corresponds to a stable adsorbate/slab system. The energy of the isolated NM molecule for this calculation is that determined for the isolated NM molecule in a cubic cell of length 12 Å. The same Brillouin-zone sampling has been used to calculate the energies of the bare slab and of the molecule-slab systems.

Representative adsorption configurations are depicted in Figures 1 and 2. For each configuration, three views are represented. The first one, denoted with the index 1, represents the initial molecular configuration at the start of the optimization process. The second and third insets, denoted with indices 2 and 3 , respectively, represent side and top views of the final adsorption configuration after full relaxation of atomic positions.

In Figure 1 we present the adsorption configurations of NM when initially the C-N bond is oriented perpendicular to the surface, with the nitro group pointing down toward the surface. Panels a1)-a3) illustrate the results obtained in which adsorption of NM takes place at an fcc site. In this case, various Al-O bonds are formed with equilibrium values between 1.897 and 2.098Å. The final (i.e., optimized) configuration, denoted as NM(**I**), represented in panels a2) and a3) illustrates marked distortions of the nitro group

due to the strong interactions of the oxygen and nitrogen atoms with the aluminum surface. As a result, the N-O bonds are significantly stretched to 1.455 and 1.476 Å, respectively, relative to the gas phase equilibrium values of 1.240 Å. Additionally, the nitro group and the C atom are no longer coplanar as in the gas phase, but in this state the molecule adopts a chair conformation. The corresponding torsional angle τ(O-O-N-C) changes from the gas phase value of 180° to -111.7° for this chemisorbed state. The large geometric changes that result upon adsorption are also reflected in a high adsorption energy. Based on Eq. (1) and the diagram level provided in Figure 3, the predicted adsorption energy is 43.3 kcal/mol.

Panels b1)-b3) of Figure 1 illustrate the case in which the initial configuration of the NM molecule interacts with an aluminum on-top site. As can be seen from the b2) and b3) images, adsorption at this site leads to complete dissociation of one of the oxygen atoms from the nitro group. The dissociated O atom adsorbs at a nearby fcc site with simultaneous bonding to three neighboring Al atoms in the first layer. The corresponding Al-O bonds are almost identical, having values between 1.85 and 1.86 Å. The remaining NM fragment, denoted N_{tr}(**I**), also chemisorbs strongly to the surface, forming bonds to aluminum via both the nitrogen atom and the remaining oxygen atom. The corresponding Al-N bond length is 1.849 Å while the Al-O bond lengths are 1.896 and 1.904 Å. As in the case of the adsorption at the fcc site, the remaining (undissociated) N-O bond of the nitroso species is significantly stretched, with a length of 1.504 Å.

In order to determine the strength of the adsorption for this nitroso complex, we have used a relation similar to that given in Eq. (1) in which E_{slab} was taken as the energy of the slab and dissociated oxygen atom complex and E_{molec} was taken to be the energy of the isolated nitrosomethane species. The specific values of the energetic levels involved are shown in Figure 3. Relative to the sum of energies of the surface with an adsorbed oxygen atom and of the isolated nitrosomethane species (see $E_{Al+O(a)+Ntr(g)}$ in Figure 3a), the adsorbed nitroso complex at the fcc site has an adsorption energy $E_{Al+O(a)+Ntr(I)}$ of 127.6-60.5=67.1 kcal/mol. This result indicates that even after cleavage of the first N-O bond, the nitroso complex also interacts strongly with the Al surface.

Finally, we present in the panels c1)-c3) the results of adsorption at an hcp surface site. In this case, both oxygen atoms of the nitro group dissociate, leading to formation of

a methylnitride chemisorbed species (denoted MeN(**I**)). The dissociated O atoms occupy fcc surface sites and form strong bonds to the Al surface. The corresponding Al-O bonds have values of 1.847, 1.847 and 1.863 Å. The longest Al-O bonds correspond to those Al atoms which are also involved in simultaneous bonding to dissociated O atoms and the N atom of the methylnitride chemisorbed species (see panel c3 in Figure 1). Likewise, the nitrogen atom in the original nitro group also forms bonds to the metal surface with Al-N bond lengths that vary from 1.926 to 1.937 Å.

The strength of the interaction of methylnitride with the surface $E_{(Al+2O(a)+MeN(I))}$-$E_{(Al+2O(a))}$-$E_{(MeN(g))}$ has been determined with respect to the sum of energies of the surface with two adsorbed oxygen atoms ($E_{Al+2O(a)}$) and that of isolated methylnitride chemisorbed species ($E_{MeN(g)}$). The corresponding energy diagram is given in Figure 3a. Based on these values we have determined the adsorption energy to be 116.1 kcal/mol for methylnitride to the surface.

In addition to the vertical adsorption configurations described above, we have also tested the case in which NM is initially oriented with the methyl group pointed toward the surface. In this case, chemisorption does not occur since the methyl group does not interact with the surface aluminum atoms. Such configurations do not lead to stable adsorption configurations and we have not investigated them further.

Beside the vertical adsorption configurations, we have also analyzed the case in which the NM molecule is initially oriented parallel to the metallic surface. We have examined three cases: the N atom of NM positioned above an Al surface atom (see panel a1, Figure 2), above an hcp site (see panel b1, Figure 2), and above an fcc site (see panel c1, Figure 2). Our calculations indicate that during the optimization of the atomic positions started from these parallel configurations, the NM molecule rotates in order to maximize the interaction of the nitro group with the aluminum surface. As a result, the molecule initially tilts such that the oxygen atoms points toward the surface. Additionally, depending on the particular molecular orientation, adsorption will take place either molecularly or dissociatively.

Panels a1)-a3) of Figure 2 illustrate a case in which dissociation does not take place, denoted as NM(**II**). In this case, rather large molecular deformations take place. As illustrated in panel a2) of Figure 2, the molecule adopts a chair configuration with the

torsional angle τ(O-O-N-C)=115.6°. The molecular C-N axis is tilted by 28° relative to the surface normal. As a result of intramolecular deformation, both the N and the O atoms of the nitro group participate in the bonding to the Al surface. In this case, the Al-O bond lengths are 1.840 Å while the Al-N bond length is 2.111 Å. The strong interaction with the metallic surface is also reflected by the stretched N-O bonds of the NM molecule, which are 1.429 Å, 0.19 Å larger than those in the gas-phase molecule. For the chemisorbed configuration with the N atom positioned above an hcp site, we find a binding energy $E_{NM(II)}$ of 53.8 kcal/mol, which is slightly larger than that found for the undissociated state in which the optimization was started from a vertical configuration of NM ($E_{NM(II)}$).

In the case where the initial configuration corresponds to the N atom above an hcp site, adsorption on the Al surface leads to dissociation of one of the N-O bonds (see panels b2 and b3 of Figure 2), with formation of chemisorbed nitrosomethane, denoted as Ntr(**II**). The dissociated O atom is adsorbed at an fcc site and forms Al-O bonds with lengths in the range 1.821-1.854 Å. The remaining O atom of the nitro group bonds to two surface Al atoms (r(Al-O)=1.877 Å and 1.938 Å), while the N atom binds at a distance of 1.865 Å to an Al surface atom. As before, an elongated N-O bond (1.523 Å) is observed. The corresponding binding energy of this nitrosomethane chemisorbed species ($E_{Ntr(II)}$) is found to be 60.1 kcal/mol, close to the value obtained for Ntr(**I**).

Finally, in the case where the N atom is initially positioned above an fcc site (panel c1, Figure 2), adsorption leads to dissociation of both O atoms. As a result, the O atoms form strong Al-O bonds (see panels c2) and c3) of Figure 1) while the remaining methylnitride chemisorbed species, denoted MeN(**II**), adsorbs perpendicular to the surface (see panel c2) of Figure 1). It is important to note that the methylnitride chemisorbed species also binds strongly to the surface. Based on the energy values represented in Figure 3 we have obtained an adsorption energy of 116.2 kcal/mol for the methylnitride chemisorbed species. This radical is bonded to the surface with Al-N bond lengths of 1.924, 1.936 and 1.936 Å.

Overall, these results indicate that NM can undergo both molecular and dissociative adsorption when deposited on the Al (111) surface. The fact that dissociation of the nitro group on the Al surface is observed in our simple energy minimizations

suggests that the activation energies of these processes are minimal. Moreover, we note that in addition to the formation of strong Al-O bonds, the dissociation products nitrosomethane or methylnitride also strongly bind to the surface through interactions of either N or O atoms.

B2. Electron Localization Function and Charge Distribution

A useful tool to investigate the nature of the chemical interaction of NM with the Al(111) surface is the electron localization function (ELF), which is defined as [21,22]

$$\mathrm{ELF}(\mathbf{r}) = \frac{1}{1+\left(\frac{\mathrm{D}(\mathbf{r})}{\mathrm{D}_h(\mathbf{r})}\right)^2} \tag{2}$$

where $\mathrm{D}(\mathbf{r})$ is the Pauli excess kinetic energy density, defined as the difference between the kinetic energy density and the von Weizsäcker kinetic energy functional

$$\mathrm{D}(\mathbf{r}) = \frac{\eta^2}{2m}\nabla_r\nabla_{r'}\rho(\vec{r},\vec{r}') - \frac{1}{4}\frac{\eta^2}{2m}\frac{|\nabla\rho(\vec{r})|^2}{\rho(\vec{r})} \tag{3}$$

and $\mathrm{D}_h(r)$ is the kinetic energy of the homogeneous electron gas for a density equal to the local density

$$\mathrm{D}_h(\mathbf{r}) = \frac{3}{5}\frac{\eta^2}{2m}\left(3\pi^2\right)^{2/3}\rho^{5/3}. \tag{4}$$

In the case of the free electron gas (Fermi gas), the value of the ELF function is by definition 0.5. Local maxima of the ELF, also called localization attractors, correspond to regions where electrons form pairs of opposite spin. Correspondingly, in the case of fully localized electrons such as lone electrons or electrons paired in a covalent bond with different spin, the ELF is close to its upper bound of unity.

Isosurfaces of ELF can be calculated and used to help explain the bonding structure and charge localization in a chemical system. A plot of the isosurface for a constant ELF=0.7 value in the case of isolated NM molecule is presented in Figure 4a. For this isosurface, several attractors can be observed in the figure: three corresponding to C-H bonds, one to the C-N bond, and two pairs of attractors on each oxygen atom corresponding to the lone pair electrons. We notice that localization is strongest in the C-H bonds and in the lone electron pairs. Figure 4 illustrates the ELF isosurfaces

corresponding to adsorption configurations of NM presented in Figure 1, namely the nondissociated state NM(**I**) (Figure 4b), the state with one O atom dissociated Ntr(**I**) (Figure 4c), and finally the state with both O atoms dissociated MeN(**I**) (Figure 4d).

For the nondissociative adsorption configuration (Figure 4b), we observe that kidney-shaped distributions on O atoms change to ring shapes, corresponding to formation of bonds to Al atoms. Also, a new attractor is present on the N atom, indicating new bonds to the substrate. In the case of the configuration with one dissociated O atom (Figure 4c), major changes are seen for the dissociated O and N atoms. In this case, there is a small charge localization on the dissociated O atom. This indicates an ionic type of bonding. Additionally, the charge localization on the N atom increases relative to the non-dissociated configuration, as indicated by the larger kidney shape attracted around this atom. Finally, in the case when both O atoms of NM dissociate, three different attractors are present around the N atom (see Figure 4d). These attractors have lobes directed towards the neighboring Al atoms. This corresponds to formation of new bonds between the methylnitride and the surface.

A common tool to provide a semi-quantitiative measure of charge transfer is the Mulliken population analysis[23] method in which the electronic charge is partitioned among the individual atoms. This partitioning has been done by using the formalism developed by Segall et al.[24] in the context of plane wave calculations as implemented in the CASTEP[25] package. Selective variations of the individual atomic Mulliken charges on O and N atoms of NM are presented in Figure 5a for the case of the isolated molecule (configuration 1) as well as for the three adsorbed states depicted in Figure 1 (configurations 2-4). The results of these calculations indicate that significant charge transfer takes place as a result of adsorption. In the case of nondissociative adsorption, there is a significant increase in the negative charge of the O atoms of about -0.3e relative to gas phase NM. A corresponding decrease of about 0.4e takes place on the positively charged N atom. Corresponding to this transfer of electrons to the NM molecule, there is an increase in the positive charge of the Al atoms bonded to the NM molecule, with values in the range 0.38-0.51e.

The process of charge transfer also occurs for the dissociative adsorption configurations. For example, in the case in which one (see configuration 3 in Figure 5a)

or both O atoms dissociate (see configuration 4 in Figure 5a), the Mulliken charges of these atoms decrease to a value of about -1e. This is accompanied by a corresponding decrease of the charge on the N atom from 0.5e for the nitroso complex to -1.0e for the methylnitride case. Simultaneously, there is a significant increase in the positive charge on the Al atoms involved in the bonding with either O atoms or with Ntr or MeN radicals, with values ranging from 0.5 to 0.88e. For the Al atoms simultaneously bonded with two O atoms or with an O and a N atom, some larger charges in the range 0.80-0.88e are observed.

Overall, these results indicate that there is a significant charge transfer from the metallic surface to the NM molecule and its radicals. Moreover, the amount of charge transferred increases with molecular dissociation. These results are consistent with the increase of the binding energy for molecular NM and its decomposition fragments to the surface.

C. FOX-7 Adsorption on Al(111) Surface.

C1. Geometries and Energies

The strong interactions of the nitro group of NM with the Al surface are likely to be present for other molecular systems containing this chemical group. In order to test this notion, we have analyzed the adsorption of another energetic molecule, namely FOX-7. This organic compound, whose synthesis was reported relatively recently,[20] is characterized as a promising high energy density material with superior shock-sensitivity properties. As in the case of NM, we have determined representative adsorption configurations of FOX-7 on the Al(111) surface for both vertical and parallel configurations, as illustrated in Figures 6 and 7, respectively. In each case we present both the initial molecular configuration at the start of the optimization process as well as the final state obtained by full optimization of the atomic coordinates.

Figure 6 shows three such sets of configurations of FOX-7 interacting with the Al(111) surface. In panel a1) the approximately planar FOX-7 molecule is initially positioned with the C=C axis perpendicular to the surface. One of the O atoms of the nitro groups is positioned approximately on top of an Al atom while the C atoms are positioned above an fcc surface site. An additional perpendicular configuration, with the C atoms of

the FOX-7 molecule positioned above an hcp site, is shown in panel b1). Finally, in panel c1) the C=C molecular axis is tilted relative to the surface normal such that both O atoms of the same nitro group interact with neighboring Al atoms.

From the results presented in panels a2) and a3) of Figure 6, we observe that adsorption takes place molecularly with binding of one of the O atoms of each nitro group to an Al atom underneath. We denote this configuration as FOX7(**I**). The Al-O distances are 1.868 Å. For this configuration, the major changes of the internal bonds are seen for the N-O bonds involved in bonding to the surface, which are stretched to about 1.35 Å. Additionally, the corresponding Al atoms where bonding takes place are raised upwards relative to the other surface atoms by about 0.33 Å. For this chemisorbed state (denoted as $E_{Al+FOX7(I)}$ in Figure 6b), the predicted binding energy is 28.4 kcal.mol. This value is smaller than the one obtained for the undissociated molecular configuration of NM(I) (see panel a2), Figure 1). This difference can be understood based on the number of direct bonds formed by the molecule to the surface. Indeed, we have noted that in the case of NM there is a significant deformation of the nitro group, which adopts a chair-type conformation such that both O and N atoms of the nitro group are involved in the bonding to the surface. For the FOX-7 molecule, however, only the O atoms participate in direct bonding, while the rest of molecular structure does not undergo any significant deformation. The lack of deformation of the FOX-7 molecule may be due in part to the intramolecular N-H...O hydrogen bonds between the amino and nitro groups. These intramolecular interactions tend to maintain the skeletal structure of the molecule.

In the case where adsorption is initiated in a vertical configuration with the C atom above an hcp site (see panel b1 in Figure 6), there is dissociative chemisorption of the FOX-7 molecule (see panels b2) and b3), Figure 6), leading to oxygen abstraction by the surface Al atoms. The dissociated O atom binds to three neighboring Al atoms, with Al-O bond lengths in the range 1.833 to1.858 Å. The remaining nitroso-FOX-7 complex (denoted as NFOX7(**I**)) tilts by 34° relative to the surface normal, thus allowing the interaction of both nitro and nitroso groups with the surface. In this case, as can be seen in panel b3) of Figure 6, both the N and O atoms of the nitroso group interact simultaneously with one of the surface atoms, denoted Al_1, forming bonds of lengths r(N-Al_1)=1.906 Å and r(O-Al_1)=1.792 Å. As a result of the strong interaction with the

molecule, this surface Al_1 atom is pulled up by 1.17 Å relative to the surface plane. A similar upward displacement is seen for the other Al atom, denoted Al_2, which is bonded to the undissociated nitro group. This atom is moved vertically by 0.81 Å.

A more quantitative measure of the interaction between the dissociated FOX-7 fragment and the Al(111) surface has been obtained by evaluation of the adsorption energy. Relative to the energy of the surface with an adsorbed oxygen atom and that of the isolated nitroso-FOX-7 radical ($E_{Al+O(a)+NFOX7(g)}$), the adsorption energy is 69.1 kcal/mol. The calculated binding energy of this radical is similar to the one of the nitroso complex of 67.1 kcal/mol in the case of nitromethane adsorption. As in the NM case, we find that after cleavage of the first N-O bond, the nitroso complex interacts strongly with the Al surface.

Finally, in the case when the initial configuration of the FOX-7 molecule is in a vertical plane but with the C=C axis tilted relative to the surface normal as illustrated in panel c1 of Figure 6, we observe that adsorption on the surface leads to dissociation of both O atoms of the same nitro group, with formation of strong Al-O bonds. The remaining FOX-7 fragment is bonded to the surface through the N-atom end (r(N-Al)=1.878 Å and 1.916 Å) and one O atom of the other nitro group (r(O-Al)=1.853 Å). The Al atom (denoted as Al1 in panel c3) in Figure 6) simultaneously bound to both N and O atoms of the FOX-7 fragment is displaced upwards relative to the surface plane by 1.38 Å. For this FOX-7 radical (denoted MFOX7(**I**)), we have estimated an adsorption energy of 160 kcal/mol. This binding energy is higher than the one of 116.1 kcal/mol obtained in the case of methylnitride chemisorbed species. The increase in binding can be understood based on the increase in the number of direct bonds formed between the FOX-7 radical and the surface. Indeed, as illustrated in Figure 6, panel c2, the FOX-7 radical is bonded to the surface through both the N atom of the dissociated nitro group as well as through one of the oxygen atoms of the other undissociated nitro group. In the methylnitride case, the bonding was only through the N atom.

In Figure 7 we present the results of atomic optimizations when the FOX-7 molecule is initially placed in a plane parallel to the surface. Two configurations have been considered: first, (see panel a1, Figure 7) one O atom of a nitro group interacts initially with a single Al atom of the surface; second, (see panel b1, Figure 7) an O atom

of a nitro group interacts simultaneously with two neighboring Al surface atoms. As in the case of NM adsorption started from a parallel configuration, the FOX-7 molecule first rotates to maximize the interaction of the nitro groups to the surface. Then, depending on the particular molecular orientation, adsorption takes place either molecularly (see panels a2 and a3, Figure 7) or dissociatively (see panels b2 and b3, Figure 7).

For the first case, shown in panels a2 and a3 of Figure 7 (denoted FOX7(**II**)), the C=C bond is tilted by about 60° relative to the normal to the surface and all four O atoms bind independently to the surface, with Al-O bond lengths in the range 1.83-1.84 Å. Additionally, the C atoms bonded to the two nitro groups forms a puckered structure (see panel a3, Figure 7) with torsional angles τ(O-O-N-C) in the range 118-122°. The values of the same angles for the gas phase structure are around 178°. The adsorption energy of this configuration is 69.5 kcal/mol. The increase in the binding energy relative to the vertical configuration described earlier (see panel a2, Figure 6) is clearly due to the fact that now there are four Al-O bonds instead of two bonds as seen previously.

Finally, adsorption initiated from a parallel configuration with simultaneous bonding of one of the O atoms to several Al surface atoms, results in dissociation of the corresponding N-O bond (see panels b2 and b3 of Figure 7). The FOX-7 radical, denoted NFOX7(**II**) again tilts relative to the surface plane such that the C=C bond makes an angle of about 57° with the surface normal. The dissociated O-atom binds to three Al surface atoms while the other O atom (denoted with O_1 in Figure 5, panel b2) of the nitro group is significantly pulled toward the H atom of the amino group (denoted with H_1 in the same figure). As a result, the corresponding intramolecular hydrogen bond distance r(O-H) decreases significantly from the gas phase value of 1.738 Å to 1.263 Å. The binding energy of this FOX-7 radical is 84.9 kcal/mol.

As in the case of NM, adsorption of FOX-7 on the Al(111) surface can lead to both molecular and dissociative configurations. For the dissociative cases, the O atoms of the nitro group embed into the surface and form strong Al-O bonds. Additionally, FOX-7 fragments bond strongly to the surface through either N or O atoms.

C2. Electron Localization Function and Charge Distribution

A comparison of the changes in the ELF isosurfaces for gas phase FOX-7 and for various adsorption configurations is presented in Figure 8. For the isolated FOX-7 molecule (see Figure 8a), several attractors can be identified. For example, the attractors corresponding to C=C, C-N and N-H bonds are clearly evident in this figure. In addition, the attractors corresponding to the lone pairs of electrons on the N atoms of the amino groups as well as on the O atoms of the nitro groups are also present. In Figure 8 we also illustrate in panels b)-d) the ELF isosurfaces corresponding to the adsorption configurations of FOX-7 shown in Figure 6, namely the molecular state (Figure 8b), the state with one O dissociated (Figure 8c) and the state with both O atoms dissociated (Figure 8d).

As in the case of molecular adsorption of NM, molecular adsorption of FOX-7 induces significant changes in the charge distributions on the O atoms. In this case, the kidney-shaped distribution seen in the gas phase on O atoms changes to a ring shape corresponding to formation of bonds to Al atoms. In the case of the configuration with one dissociated O atom (Figure 8c), the most pronounced changes in charge distribution are seen for the O and N atoms involved in dissociation. There is little localization of charge on the dissociated O atom, indicative of ionic bonding. However, charge localization on the N atom of the nitro group where dissociation takes place increases significantly such that now a new attractor is present on this atom (see Figure 8c). Finally, in the case where both O atoms of FOX-7 dissociate, two different attractors are now present around the N atom, as shown in Figure 8d. These lobes are directed towards the two neighboring Al atoms and correspond to formation of new bonds between the FOX-7 radical and the metallic surface.

As in the case of NM adsorption, the most important charge variations take place on the nitro group of the FOX-7 molecule involved in direct bonding to the surface. The corresponding variation of the Mulliken charges on the corresponding the N and O atom are presented in Figure 5b. Here we have considered the case of isolated molecule (configuration 1) as well as of the chemisorbed states illustrated in Figure 6 (configurations 2-4). The overall trend seen for the FOX-7 molecule is similar to that observed for NM (see Figure 5a). Namely, as a result of either molecular or dissociative adsorption on the surface, there is a significant electronic charge transfer from the surface

to the molecule. The amount of charge transferred increases in the order: molecular adsorbed state (configuration 2) → dissociative state with one dissociated O atom (configuration 3) → dissociative state with both O atoms dissociated (configuration 4). As shown in Figure 5b, there is a continuous decrease of the charges on both N and O atoms when going from configuration 2 to configuration 4. In the case of configuration 4 of Figure 5b, the charges on dissociated O atoms as well as on the N atom of the nitro group involved in dissociation are about -1e. Corresponding to this transfer of electrons to the FOX-7 molecule, there is a corresponding increase in the positive charge of the Al atoms bonded either to the dissociated O atoms or to the remaining FOX-7 fragment. For example, the Al atoms bonded with a single O atom have charges in the range 0.38-0.46e. This positive charge increases to 0.94e on the Al atoms bonded simultaneously with two O atoms. The largest charge increase is seen for those Al atoms that are bonded simultaneously to O and N atoms, namely atoms denoted with Al_1 in Figure 6, panels b2 and c2. The corresponding charges on these atoms are 1.26e and 1.41e. Overall, as in the case of NM, the increase in the amount of charge transferred to the adsorbed molecule or its dissociation fragments is directly correlated to the increase in the corresponding binding energy.

IV. Conclusions

The interactions of NM and FOX-7 molecules with the Al(111) surface have been investigated based on optimizations performed using spin-polarized GGA plane-wave density functional theory calculations. The main objective of this study was to determine the possible reaction mechanisms at the molecule-metallic surface interface. The results of our calculations indicate a common propensity for oxidation of the aluminum surface by the oxygen-rich nitro groups (NO_2) of the NM and FOX-7 molecules. Dissociation of the nitro groups and formation of strong Al-O bonds appears to be a common mechanism for these molecules. Additionally, we have found that both the molecular adsorption as well as the dissociation processes takes place with significant charge redistribution. These large charge redistributions have been found to be consistent with the strong binding energies for the dissociated O atoms and for the dissociation fragments of either NM or FOX-7 molecules. These results suggest

that contact between nitro-containing energetic compounds and A1 metal will result in rapid oxidation reactions.

Acknowledgements

The authors gratefully acknowledge grants of computer time at the Army Research Laboratory, Aeronautical System Center, and the Naval Oceanographic Office Major Shared Resource Centers, sponsored by the Department of Defense High Performance Computing Modernization Program. Donald L. Thompson gratefully acknowledges support by the U.S. Army Research Office under grant number DAAD 19-01-1-0503.

References

1. Sutton, G. P., "*Rocket Propulsion Elements*", John Wiley & Sons, Inc., 1992.
2. Kwok, Q. S. M.; Fouchard, R. C.; Turcotte, A.M.; Lightfoot, P.D.; Bowes, R. Propellants, Explosives, Pyrotechnics **2002**, 27, 229.
3. Ivanov, G. V.; Tepper, F. in "*Challenges in Propellants and Combustion 100 Years After Nobel*", K. K. Kuo (Eds), Begell House, New York 1997, p.636.
4. Wilson, W. H.; Kramer, M. P. in Proceedings of the High Energy Density Matter (HEDM) Contractors Conference, Ed. M. R. Berman, 24-26 Oct. 2002, Park City, UT.
5. Kresse, G.; Hafner, J. *Phys. Rev.* **1993**, B 48, 13115.
6. Kresse, G. ; Furthmüller, J. *Comput. Mat. Sci.* **1996**, 6, 15.
7. Kresse, G.; Furthmüller, J. *Phys. Rev.* **1996**, B 54, 11169.
8. Vanderbilt, D. *Phys. Rev.* **1990**, B 41, 7892.
9. Kresse, G; Hafner, J. *J. Phys. Condens. Matter* **1994**, 6, 824.
10. Perdew, J. P.; Chevary, J. A.; Vosko, S. H.; Jackson, K. A.; Pedersen, M. R.; Singh, D. J.; Frolhais, C. *Phys. Rev.* **1992**, B 46, 6671.
11. Monkhorst, H. J.; Pack, J. D. *Phys. Rev.* **1976**, B 13, 5188.
12. Methfessel, M.; Paxton, A. T. *Phys. Rev.* **1989**, B40, 3616.
13. Kresse, G; Hafner, J. *Phys. Rev.* **1993**, B 47, 588.
14. Murnaghan, F. D. *Proc. Natl. Acad. Sci USA* **1944**, 30, 2344.
15. King, H. W., in *CRC Handbook of Chemistry and Physics*, 81st ed., edited by David R. Linde, CRC Press, Boca Raton, FL, 2000.
16. Gaudoin, R.; Foulkes, W. M. C. Phys. Rev. **2002**, B66, 052104.
17. Sorescu, D. C.; Rice, B. M. Rice; Thompson, D. L. J. Phys. Chem. B **2000**, 104, 8406.
18. See section 9 in *CRC Handbook of Chemistry and Physics*, 81st ed., edited by David R. Linde, CRC Press, Boca Raton, FL, 2000.
19. Sorescu, D. C.; Boatz, J.A.; Thompson, D. L. *J. Phys. Chem.* A **2001**, 105, 5010.
20. Latypov, N. V.; Bergman, J.; Langlet, A.; Wellmar, U.; Bemm U. *Tetrahedron* **1998**, 54, 11525.
21. Silvi, A.; Savin, A. *Nature* **1994,** 371, 683.

22. Savin A.; Nesper, R.; Wengert, S.; Fässler, *Angew. Chem. Int. Engl.* **1997**, 36, 1808.

23. Mulliken, R. S. *J. Chem. Phys.* **1955**, 23, 1833, 2343.

24. Segall, M. D.; Pickard, C. J.; Shah, R.; Payne, M. C. *Phys. Rev.* **1996**, B54, 16317.

25. Milman, V.; Winkler, B.; White, J. A.; Pickard, C. J.; Payne, M. C.; Akhmatskaya, E. V.; Nobes, R. H. *Int. J. Quantum Chem.* **2000**, 77, 895.

FIGURE CAPTIONS

Figure 1. Adsorption configurations of NM on the Al(111) surface obtained from initial vertical configurations: (a) N above a fcc site (NM(**I**)); (b) N above on-top site (Ntr(**I**)); (c) N above an hcp site (MeN(**I**)). The initial configurations are depicted in panels a1-c1 while the lateral and top views of the corresponding final configurations are shown in panels a2-c2 and a3-c3, respectively.

Figure 2. Adsorption configurations of NM on the Al(111) surface obtained from initial parallel configurations: (a) N above a top site (NM(**II**)); (b) N above an hcp site (Ntr(**II**)); (c) N above a fcc site (MeN(**II**)). The initial configurations are depicted in panels a1-c1 while the lateral and top views of the corresponding final configurations are shown in panels a2-c2 and a3-c3, respectively.

Figure 3. Relative energies of various configurations of NM (a) and FOX-7 (b) adsorbed on the Al(111) surface as described in text. The abbreviations used corresponding to: h – horizontal configuration, v – vertical configuration, a – adsorbed configuration, g –gas phase configuration. The other abbreviations NM(I), NM(II), Ntr(I), Ntr(II), MeN(I), MeN(II), FOX7(I), FOX7(II), NFOX7(I), NFOX7(II), MFOX7(I) are described in the text.

Figure 4. Comparison of the isosurfaces of the electron localization function (ELF=0.7) for (a) NM in the gas phase; (b) NM molecularly adsorbed (NM(**I**)); (c) NM dissociatively adsorbed with one O atom dissociated (Ntr(**I**)); (d) NM dissociatively adsorbed with both O atoms dissociated (MeN(**I**)). Configurations (b)-(d) correspond to the same structures shownin Figure 1.

Figure 5. Variation of the Mulliken charges on the individual atoms of the nitro group for (a) NM and (b) FOX-7. In both cases configuration 1 corresponds to gas phase molecules, while configurations 2-4 correspond to the molecular adsorption state, dissociative adsorption state with one O dissociated, and dissociative adsorption state with both O

dissociated, respectively. These configurations are those depicted in Figure 1 for NM and in Figure 6 for FOX-7.

Figure 6. Adsorption configurations of FOX-7 on the Al(111) surface obtained from initial vertical configurations: (a) C atom above a fcc site (FOX7(**I**)); (b) C above an hcp site (NFOX7(**I**)); (c) N above an hcp site (MFOX7(**I**)). The initial configurations are depicted in panels a1-c1 while the lateral and top views of the corresponding final configurations are presented in panels a2-c2 and a3-c3, respectively.

Figure 7. Adsorption configurations of FOX-7 on the Al(111) surface obtained from initial parallel configurations: (a) O atom interacts with a single Al atom (FOX7(**II**)); (b) O atom interacts simultaneously with two Al atoms (MFOX7(**II**)). The initial configurations are depicted in panels a1-c1 while the lateral and top views of the corresponding final configurations are presented in panels a2-c2 and a3-c3, respectively.

Figure 8. Comparison of the isosurfaces of the electron localization function (ELF=0.7) for (a) FOX-7 in the gas phase; (b) FOX-7 molecularly adsorbed (FOX7(**I**)); (c) FOX-7 dissociatively adsorbed with one O atom dissociated (NFOX7(**I**)); (d) FOX-7 dissociatively adsorbed with both O atoms dissociated (MFOX7(**I**)). Configurations (b)-(d) correspond to the same structures as shown in Figure 4.

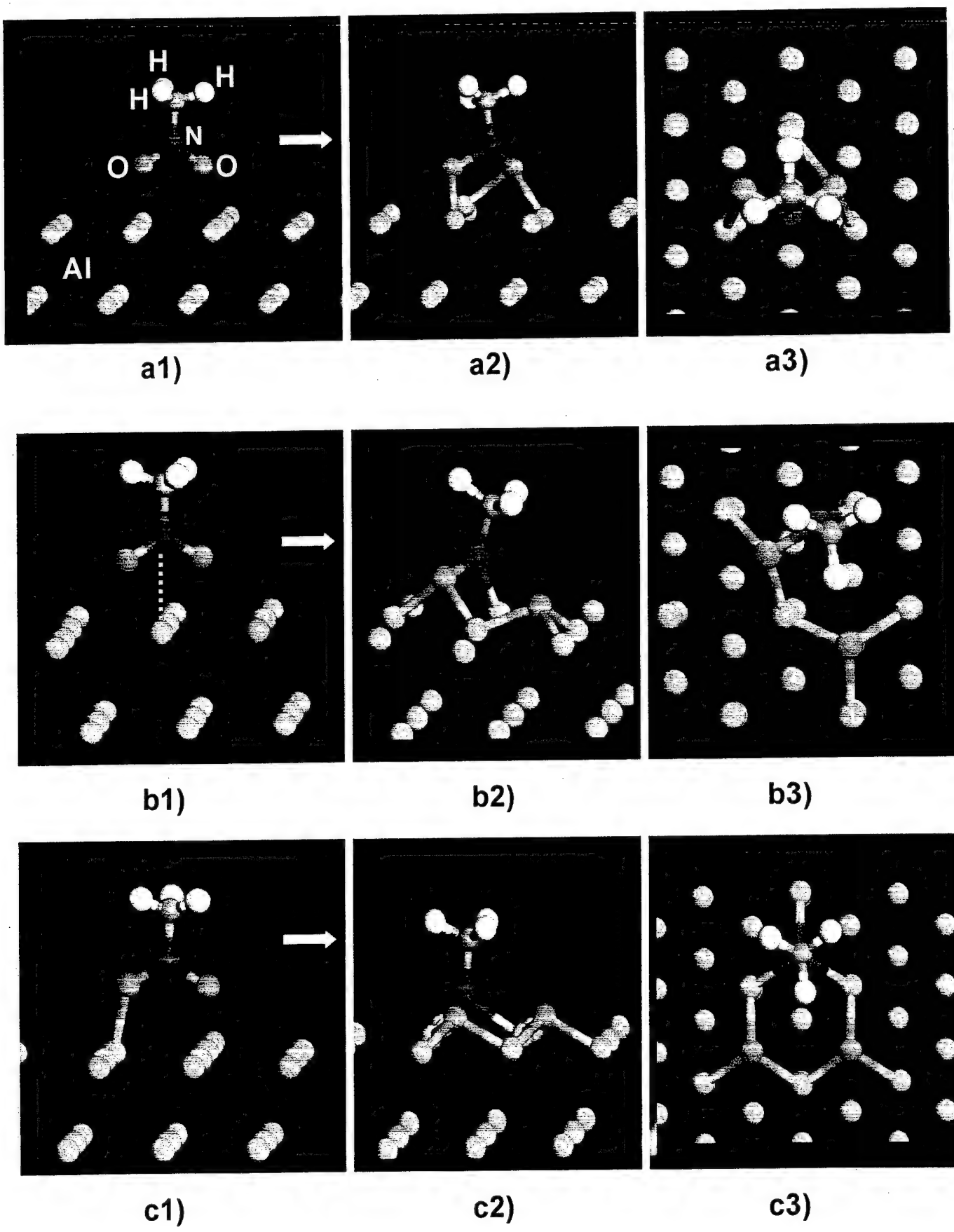

Figure 1

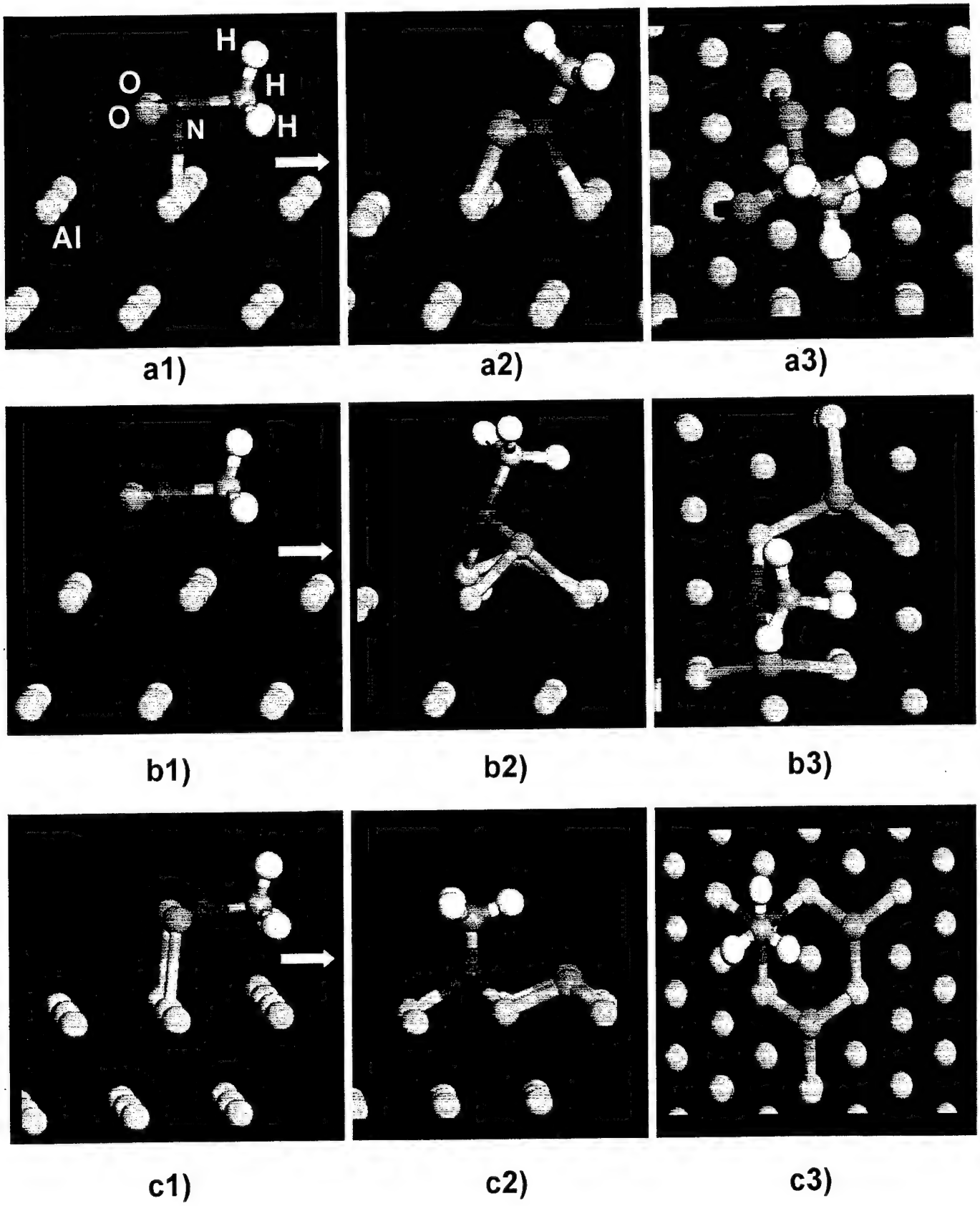

Figure 2

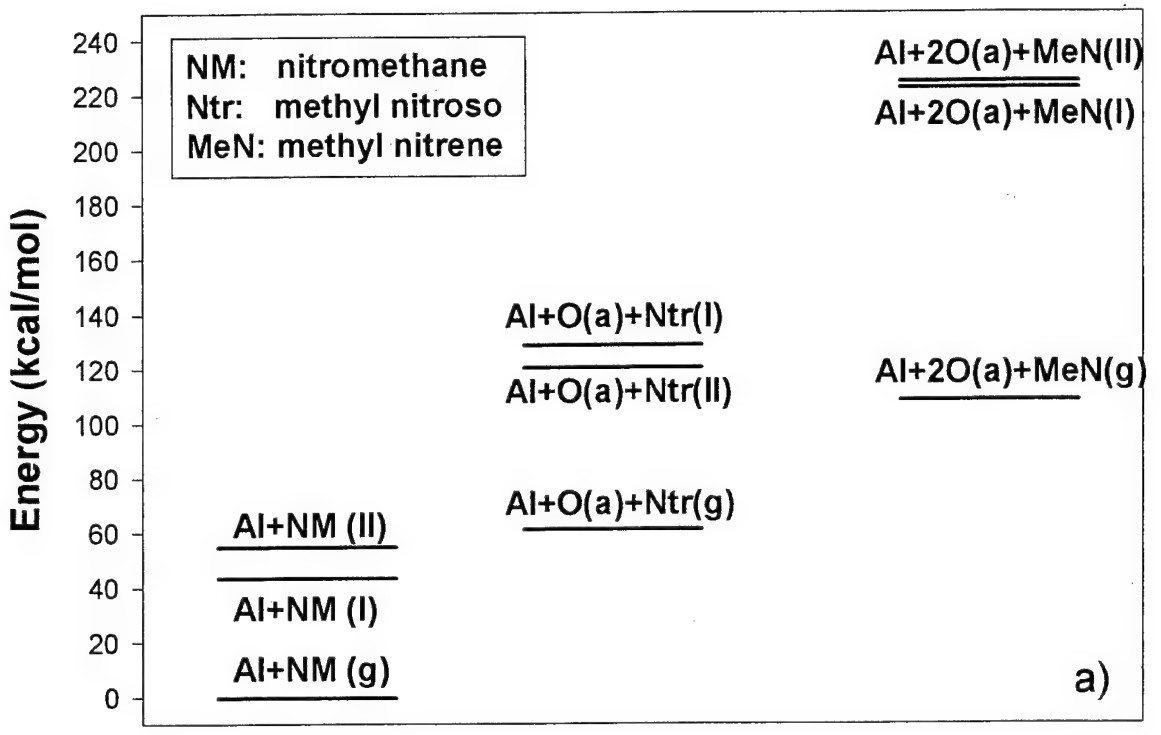
Energy (kcal/mol)
240
220
200
180
160
140
120
100
80
60
40
20
0
NM: nitromethane
Ntr: methyl nitroso
MeN: methyl nitrene
Al+2O(a)+MeN(II)
Al+2O(a)+MeN(I)
Al+O(a)+Ntr(I)
Al+O(a)+Ntr(II)
Al+2O(a)+MeN(g)
Al+O(a)+Ntr(g)
Al+NM (II)
Al+NM (I)
Al+NM (g)
a)

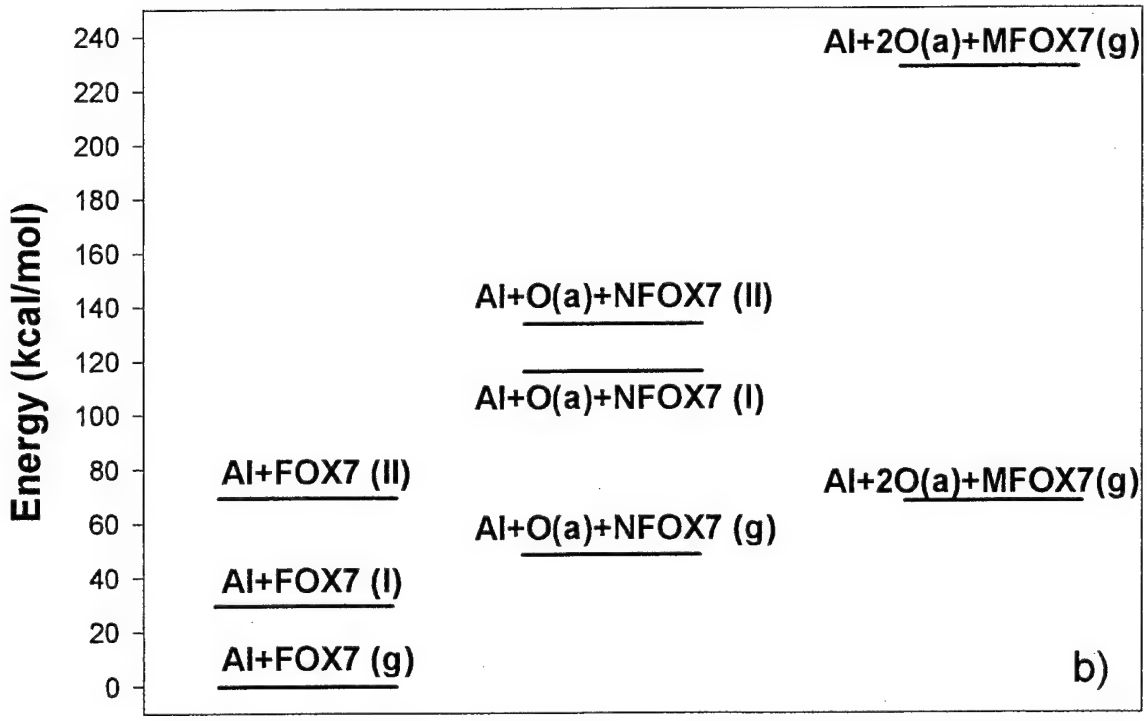
Energy (kcal/mol)
240
220
200
180
160
140
120
100
80
60
40
20
0
Al+2O(a)+MFOX7(g)
Al+O(a)+NFOX7 (II)
Al+O(a)+NFOX7 (I)
Al+FOX7 (II)
Al+2O(a)+MFOX7(g)
Al+O(a)+NFOX7 (g)
Al+FOX7 (I)
Al+FOX7 (g)
b)

Figure 3

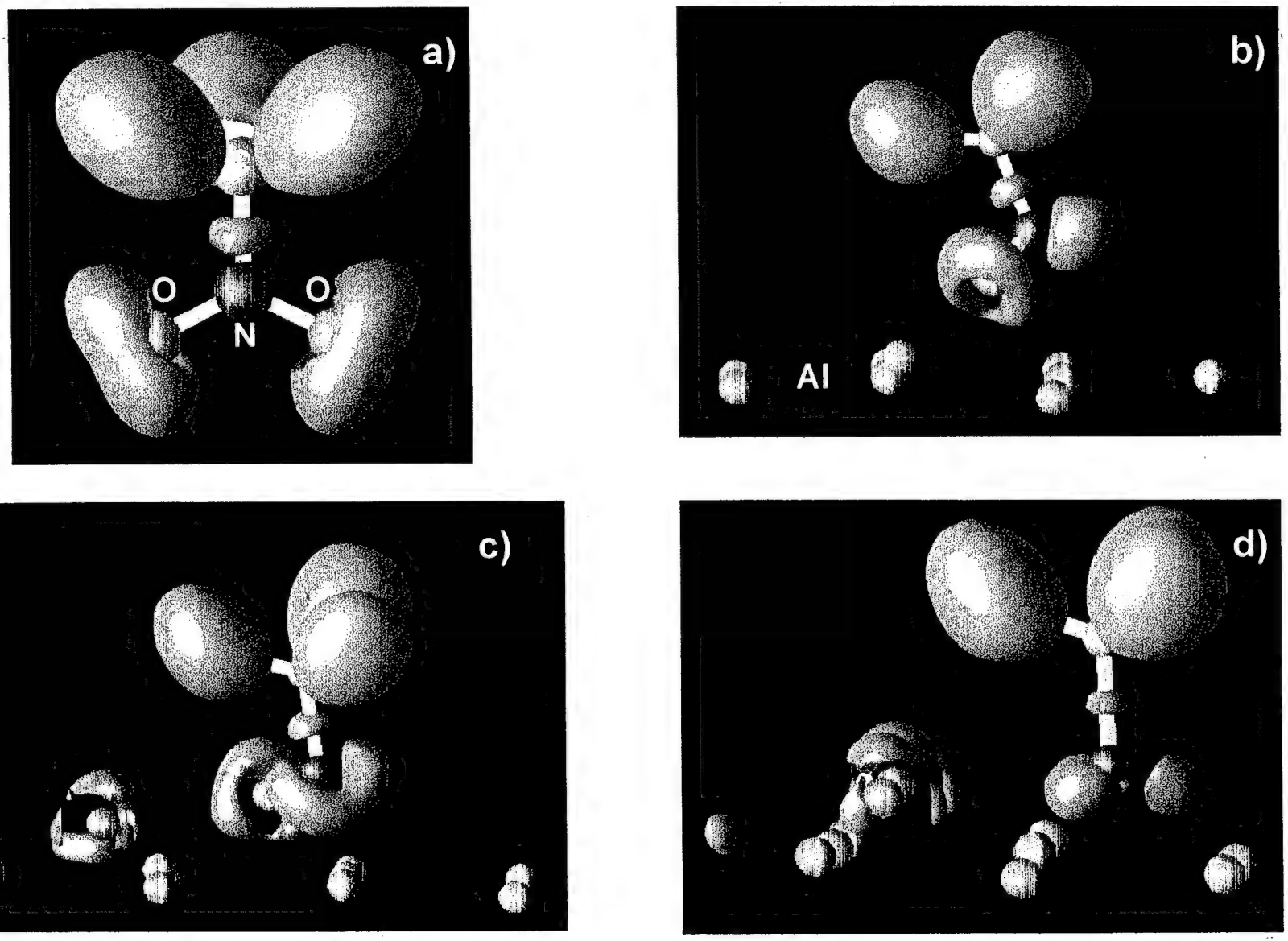

Figure 4

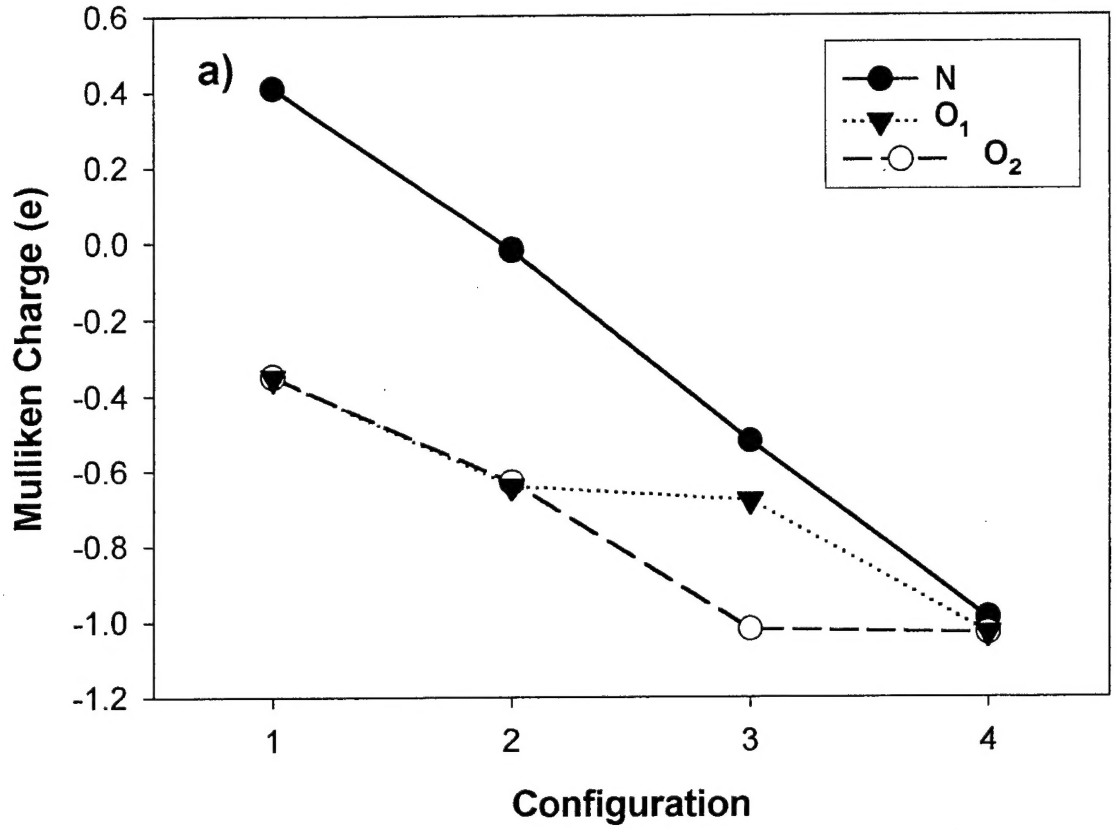
a)
N
O_1
O_2
Mulliken Charge (e)
0.6
0.4
0.2
0.0
-0.2
-0.4
-0.6
-0.8
-1.0
-1.2
1
2
3
4
Configuration

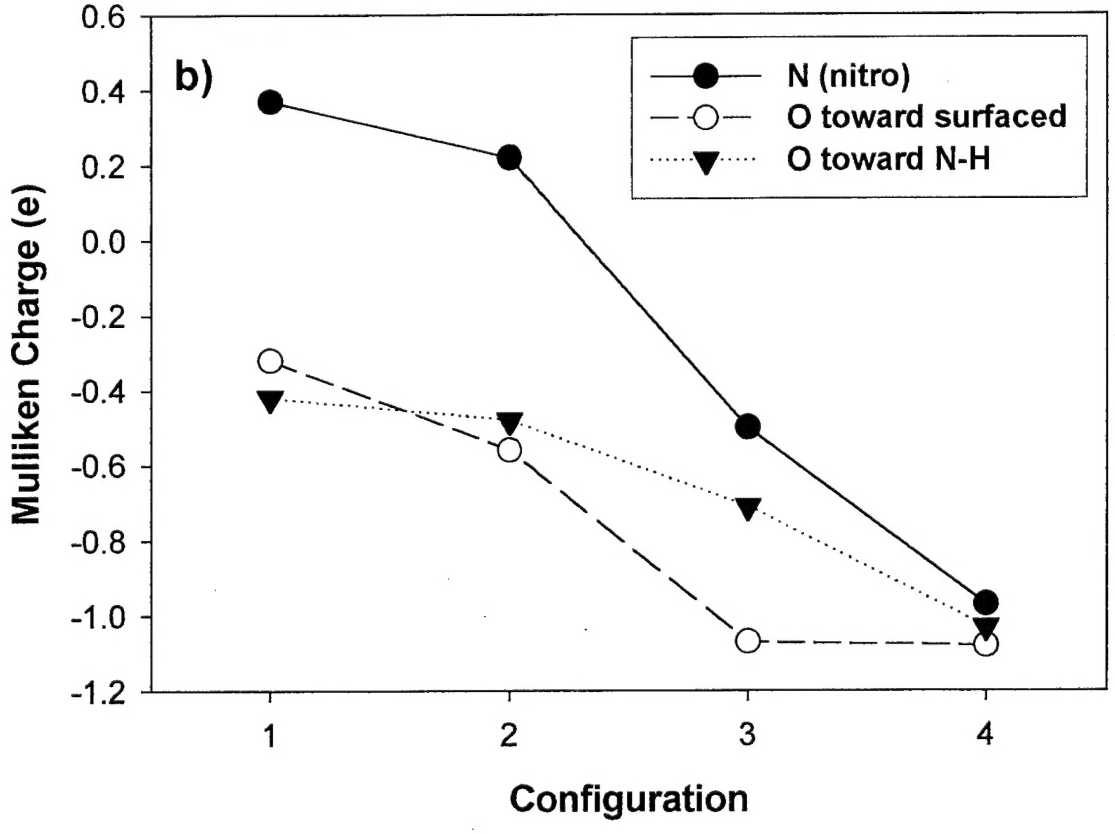
b)
N (nitro)
O toward surfaced
O toward N-H
Mulliken Charge (e)
0.6
0.4
0.2
0.0
-0.2
-0.4
-0.6
-0.8
-1.0
-1.2
1
2
3
4
Configuration

Figure 5

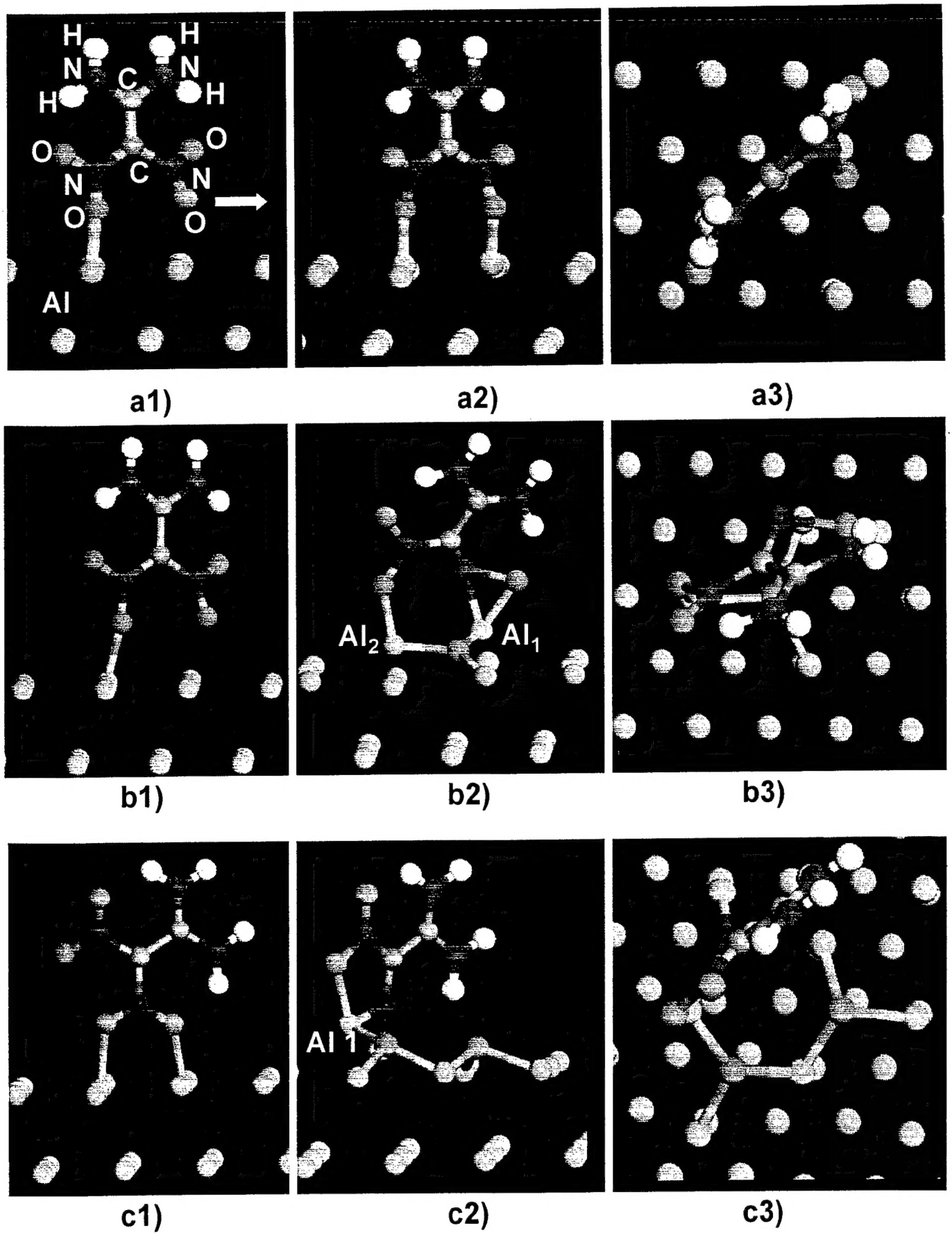

Figure 6

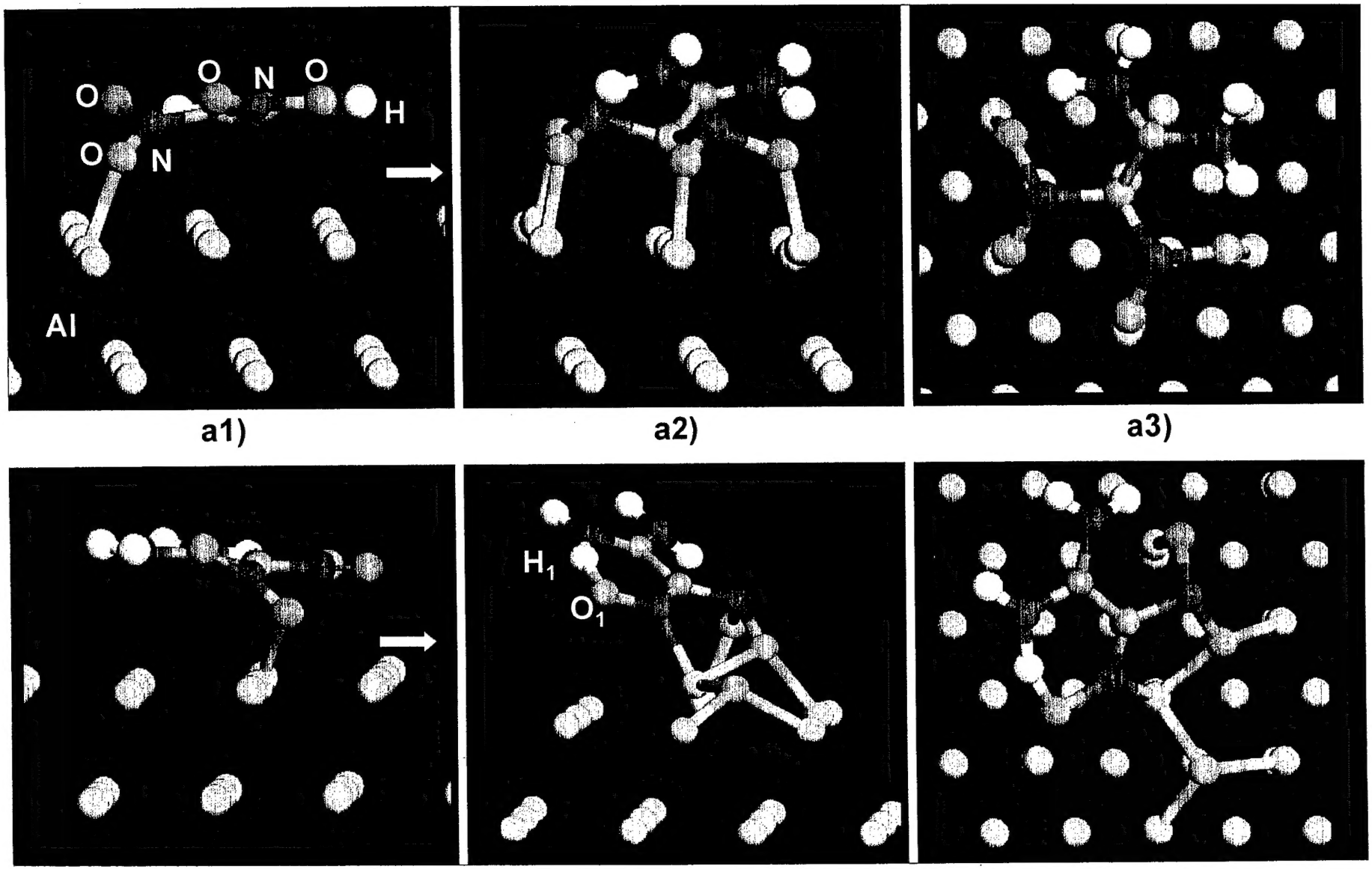

Figure 7

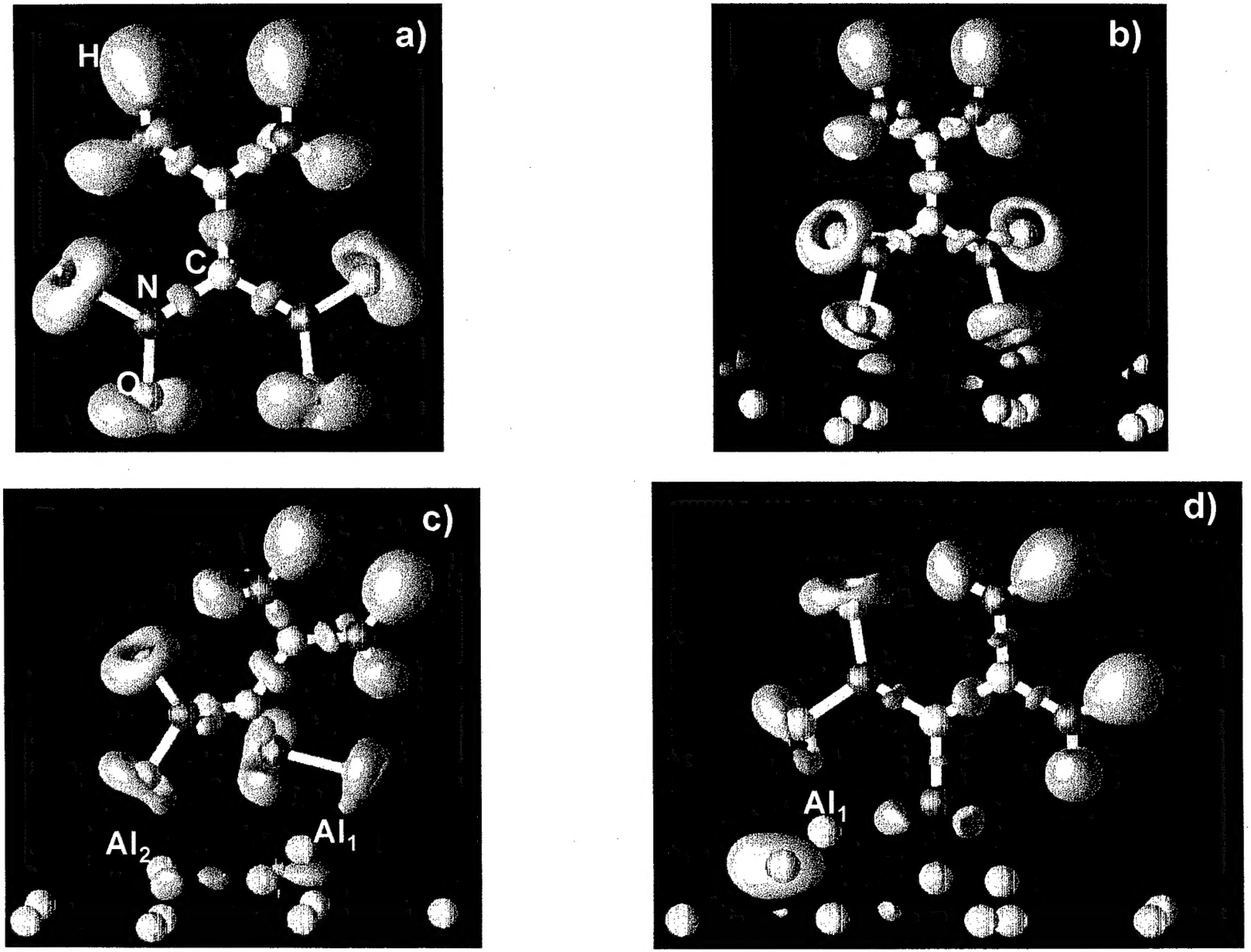

Figure 8